LBL-19359
Preprint c.2

Lawrence Berkeley Laboratory
UNIVERSITY OF CALIFORNIA

Materials & Molecular Research Division

LAWRENCE
BERKELEY LABORATORY
1986
LIBRARY AND

Submitted to Journal of
the Electrochemical Society

OXYGEN ACTIVITY AND ASYMMETRIC POLARIZATION AT THE SODIUM/BETA"-ALUMINA INTERFACE

C. Mailhe, S. Visco, and L. De Jonghe

November 1985

TWO-WEEK LOAN COPY
This is a Library Circulating Copy
which may be borrowed for two weeks.

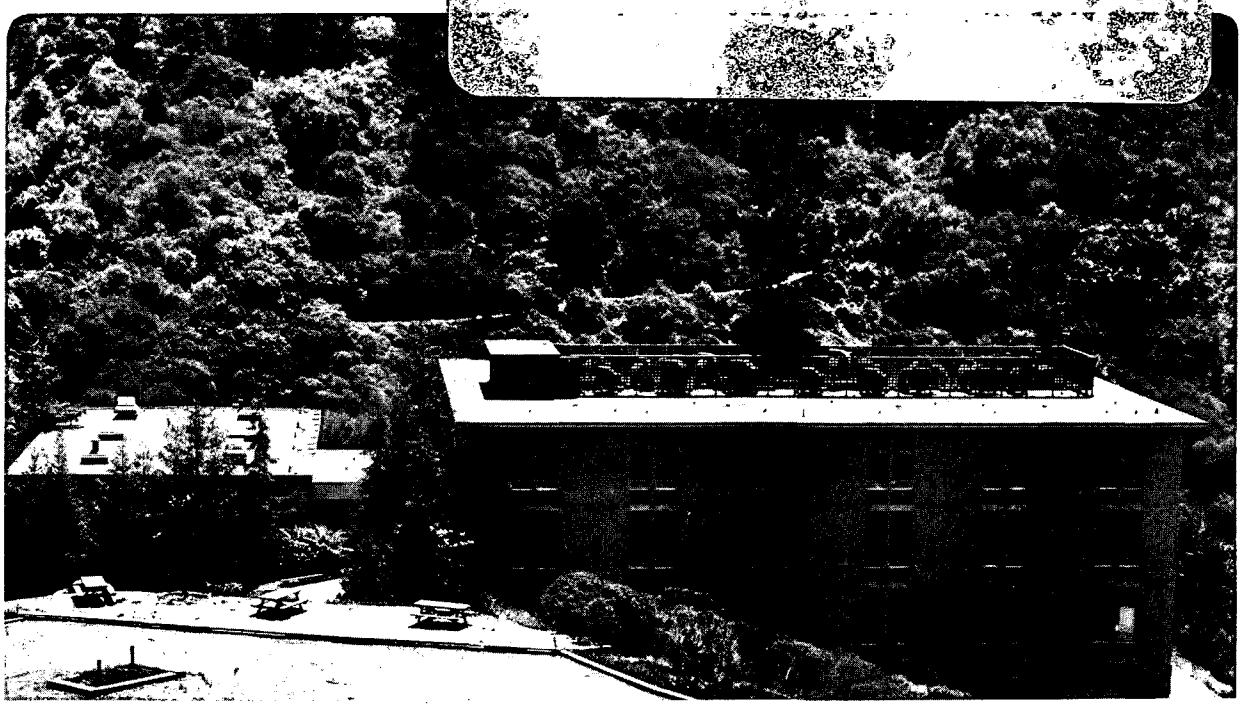

LBL-19359 c.2

Prepared for the U.S. Department of Energy under Contract DE-AC03-76SF00098

DISCLAIMER

This document was prepared as an account of work sponsored by the United States Government. While this document is believed to contain correct information, neither the United States Government nor any agency thereof, nor the Regents of the University of California, nor any of their employees, makes any warranty, express or implied, or assumes any legal responsibility for the accuracy, completeness, or usefulness of any information, apparatus, product, or process disclosed, or represents that its use would not infringe privately owned rights. Reference herein to any specific commercial product, process, or service by its trade name, trademark, manufacturer, or otherwise, does not necessarily constitute or imply its endorsement, recommendation, or favoring by the United States Government or any agency thereof, or the Regents of the University of California. The views and opinions of authors expressed herein do not necessarily state or reflect those of the United States Government or any agency thereof or the Regents of the University of California.

OXYGEN ACTIVITY AND ASYMMETRIC POLARIZATION AT THE SODIUM/BETA"-ALUMINA INTERFACE

Catherine Mailhe, Steve Visco and Lutgard De Jonghe

Lawrence Berkeley Laboratory
Materials and Molecular Research
University of California
Berkeley, CA 94720

Abstract

Asymmetric polarization at the sodium/beta"-alumina interface during ionic charge transfer has been studied using cyclic voltammetry with Na/beta"-alumina/Na cells. It was found that contamination of the sodium electrode by oxygen, as O_2 or H_2O, causes asymmetric polarization. Polarization is quite severe in the range of 150-200^0 C, and is attributed to the presence of an adsorbed oxide film. The adsorption/desorption behavior of the resistive film could be described by a simple Langmuir model. Asymmetric polarization can be eliminated by lowering the oxide content of the sodium electrode to levels such that adsorption is negligible. This is achieved by the use of carefully dried electrolyte tubes with either electrolytically generated sodium, or sodium from which the oxygen has been scavenged with Ti sponge.

This work was supported by the Assistant Secretary for Conservation and Renewables, Office of Advanced Conservation Technology, Electrochemical Systems Research Division of the U. S. Department of Energy under Contract No. DE-AC03-76SF000098.

INTRODUCTION

Asymmetric charge transfer resistance with dc ionic current flow at the sodium/beta"-alumina interface has been reported by several workers (1-6). Significant asymmetric polarization can be harmful to the efficiency of battery operation, and is associated with early electroyte failure.

The increasing resistance at the electrode/electrolyte interface during sodium discharge has been attributed to the existence of a thin, passivating film (1,2). The extent and time dependence of the asymmetry seems to depend on the composition of sodium-beta"-alumina electrolyte. It has also been observed that heating to 350°C both improves the wetting of beta"-alumina by sodium and decreases the interface polarization. It has been proposed that this may reflect the increased solubility of Na_2O at higher temperatures (1). The general behavior of the charge - transfer resistance therefore indicates that the oxygen content of the sodium electrode maybe an important parameter in the Na/S cell operation. In the present paper the role of oxygen dissolved in the molten sodium electrode and the associated interface polarization are examined. A method is described for controlling the oxygen fugacity, and a means for eliminating the asymmetric polarization is presented.

Solubility of Oxygen in Sodium - The effects of dissolved impurities in liquid sodium on its corrosive properties have been examined extensively (7-9). The solubilites of Na_2O, NaOH, and NaH in liquid sodium as a function of temperature are known (10).

For example, the Na-O-H equilibria data show that the solubility of oxide in sodium is larger if the source of contamination is H_2O as opposed to O_2 (Table 1). The rate of dissolution of Na_2O in molten sodium, k_d, has also been determined for the reaction

$$Na_2O \text{ (solid)} \longrightarrow 2Na + [O] \text{ (in solution)}$$

as a function of temperature (11). The rate of precipitation (k_a) can then be calculated from the equilibrium constants. As expected, the rate of dissolution is many orders of magnitude lower than the rate of precipitation. Therefore, any Na_2O precipitated at the sodium/beta"-alumina interface due to local changes in oxygen concentration may persist until it slowly redissolves to establish bulk equilibrium.

The presence of sodium oxide dispersed in the liquid sodium electrode and/or adhering as a resistive film to the surface of the electrolyte can be expected to affect significantly the wetting of the electrolyte. Early investigations of the surface tension of liquid sodium were systematically high due to the presence of impurities, and it has been reported that traces of oxygen will increase the surface tension of molten sodium (12). This indicates great care should be exercised in using pure sodium, since increased surface tension means poorer wetting of the solid electrolyte. In fact, the numerical difference in measured surface tension of liquid sodium between the previously and currently accepted values (obtained with very pure sodium) is as large as the change in surface tension between 150°C and 300°C. This implies that the presence of impurities,

particularly oxygen or water, may play as important a role as temperature in the wetting of sodium beta"-alumina by sodium. This assertion is supported by the observation on the Dow Na/S cell that limiting the oxide (and calcium) content of the sodium to a few ppm results in extrememly good wetting of the glass solid electrolyte (13).

The presence of excess oxygen in the liquid sodium anode presents another potential problem: as the cell is discharged, the concentration of oxygen in the remaining sodium (at the sodium/electrolyte interface) may exceed the solubility limit, leading to the deposition of $Na_2O(s)$ of unit activity. This might potentially lead to corrosion of the electrolyte by the reaction

$$3Na_2O(s) + 3Al_2O_3(s) \rightarrow 6NaAlO_2(s) \quad = -554 \text{ kj/mol}$$

Also, high concentrations of Na_2O or NaOH in liquid sodium are known to be very corrosive towards many materials, e.g. stainless steel (10).

The above discussion illustrates the importance of proper control of the oxygen fugacity in the molten sodium anode in the Na/S battery. Commercial sodium typically contains 1000 to 2000 ppm impurities and is almost always saturated with oxygen. Table 1 shows that the solubility of Na_2O in liquid sodium falls from 215 ppmO at 350 C to 1 ppmO at 120°C. Therefore, efficient filtering at 120°C can possibly reduce the oxygen contamination to approximately 1 ppmO. It has also been reported that vacuum distillation of sodium can yield 99.995% pure (5 ppm impurities) sodium. Alternatively, one can electrolyse sodium through the

beta"-alumina electrolyte, and be limited in sodium purity only by the purity of the atmosphere in which the electrolysis was performed. However, even if the sodium anode is initially meticulously purified, there are sources of contamination, such as leaks in the cell seals, moisture intercalated into the bulk of the electrolyte, adsorbed O_2 or H_2O on the electrolyte surface, etc. In order to maintain the oxide activity in the sodium electrode at a level consistent with optimal cell performance, it is proposed to introduce into the sodium electrode a metal thermodynamically capable of reducing Na_2O to sodium metal, without destructively reducing the electrolyte itself. The reaction $M + Na_2O \longrightarrow Na + M_xO_y$ must occur at a kinetically acceptable rate at the temperature of operation of the cell, and produce an insoluble oxide M_xO_y.

Titanium metal is capable of reducing Na_2O in the required temperature range, and its effect on the electrochemical behavior of the sodium/beta"-alumina interface is reported in this investigation. Several other metals are thermodynamically capable of reducing Na_2O in the required temperature range including V, Zr, U, Al, and Mn. These metals and their oxides are reported to be practically insoluble in the temperature range of interest (9).

The activity of oxide in molten sodium, A_o, can be estimated from the Henry's Law aproximation as

$$A_o = X_o/X_{sat}$$

where X_o is the mole fraction of dissolved oxide, and X_{sat} is the

mole fraction at saturation. The oxygen chemical potential for different oxide concentrations can be calculated accordingly. For example, the intersection of the oxygen fugacity of sodium oxide with that of titanium oxide occurs at 0.0001 ppmO, at 350°C.

Therefore, if the reaction rate with titanium is sufficiently fast, the oxygen concentration will be maintained at 0.0001ppm(O) at 350°C, at least until the available surface of the titanium metal is completely oxidized, and provided that TiO_2 is sufficiently insoluble in sodium. In order to have the maximum amount of surface area available for reaction, titanium sponge is utilized in this investigation.

EXPERIMENTAL

Electrochemical cells were designed to facilitate the characterization of the sodium/beta"-alumina interface. The electrolytes used were tubes of sodium-beta"-alumina supplied by Ceramatec, Inc., Salt Lake City, Utah. To keep the electrolyte tubes positioned properly in the cell, alpha-alumina disks were glass-sealed to the tubes.

The experimental Na/Na cell design is shown in fig. 1. The electrochemical measurements were made with a four-electrode system. A nickel working electrode (WE) was placed in the center of the electrolyte tube, making contact with the bottom of the tube via a fine nickel wire spool (necessary for the experiments in which electrolytic sodium is used). The electrolyte tube was immersed in molten sodium in contact with the stainless steel

body of the cell, which served as the counter electrode (CE). A third nickel wire electrode was positioned in contact with the top of the electrolyte tube, and a sufficient current was passed through it to produce a small droplet of sodium. This established a reference electrode (RE). The fourth electrode consisted of a non-current carrying potential probe attached to the WE. This allowed correcting for possible contact resistances at the current-carrying working electrode.

The cells were assembled in a dry box under an argon atmosphere with less than 1 ppm of O_2 and H_2O. The sodium used for the counter electrode side of the Na/Na cell was filtered through stainless steel wool at 150°C to remove some of the bulk oxides. The sodium was undoubtably still saturated with oxygen. About 100 grams of this sodium was poured into the stainless steel body of the cell and the electrolyte tube was then carefully placed into the molten sodium. The electrolyte tube was then filled with pre-treated sodium and, in some tests enough solid Na_2O_2 to saturate the sodium electrode. If electrolytic sodium was to be used as the working electrode, sodium was not added to the inside of the electrolyte tube, but later electrolized into the tube. Finally, the top of the cell body (containing the WE and RE) was positioned and fastened down against a copper gasket to make a hermetic seal. All experiments could then be carried out in a furnace with an air atmosphere. The temperature range used for the experiments was between 160°C and 350°C.

Electrochemical measurements were made with a 173 Potentiostat/Galvanostat in conjunction with a Universal Programmer (Princeton Aplied Research, Princeton, New Jersey). The potential (with respect to the RE) of the fourth probe was scanned as a function of current passed across the cell, using triangular wave cyclic voltammetry, and the resulting current-potential curves were recorded.

The simplified equivalent circuit for the Na/Na cells used in this investigation is shown in Fig. 2. The potential drop measured between the potential probe and the reference electrode (RE) includes the potential drop across part of the beta"-alumina electrolyte and across the inner sodium/beta"-alumina interface. Assuming that the bulk resistance of the electrolyte doesn't change over the course of the experiment, any deviations from ohmic behavior of the cell current as the potential is cycled (the capacitive and inductive current in these experiments is negligible), implies changes in the inside interfacial resistance, R_i. Thus changes in the resistance at the inner interface of these cells, manifested as an asymmetric polarization, were found as a function of experimental conditions. To simplify the interpretation of the experimental current-potential curves, the resistances were calculated from the IR drop between the RE and the potential probe, and the corresponding resistance-potential curves were plotted.

It was found that the virtual position of the reference electrode is determined by the relative levels of the sodium electrodes inside and outside of the tube. Therefore, the

fraction of the voltage drop due to the total electrolyte resistance is set by the relative positions of the sodium electrodes. Once the virtual position of the reference electrode is established, it does not move over the course of the experiment since the sodium levels did not change appreciably.

To assess the effects of oxide concentration on the electrochemical behavior of the sodium/beta" interface, the working electrode used in the following experiments was composed of sodium with various oxygen contents:

A. Electrolytically "pure" sodium.

B. Electrolytic sodium saturated with Na_2O.

C. Reagent grade sodium filtered at 150°C through stainless steel wool.

D. Sodium filtered as above and titanium sponge added.

E. Sodium filtered as above and then reacted with titanium sponge at 350°C for 24 hours and refiltered at 150°C. Some additional Ti was then added.

F. Electrolyte tube exposed to atmospheric moisture for two weeks (in all other experiments the electrolyte tubes were baked out under vacuum).

RESULTS

High Temperature (300 - 350°C): - In almost every case, the Na/Na cells cycled at high temperatures showed no asymmetric polarization; the current-potential curves simply exhibited linear ohmic behavior. The only cells which exhibited measurable polarization were ones in which the electrolyte tubes

were exposed to moisture, or in which the electrolyte tubes were not baked out under vacuum. Current-potential and resistance-potential curves for this case are shown in Figures 3a and 3b. As can be seen from Fig. 3b, the resistance at the inside interface, R_i, increases as sodium is discharged flowing out of the electrolyte tube, and decreases as sodium is electrolysed into the tube. If the maximum change in the interface resistance is taken to be the difference between the high and low values from the resistance-potential curves, one can see that the resistance at the inner sodium/beta"-alumina interface changes by 18 milliohms over the range of potentials scanned. Also evident is that the polarization is much more severe at low scan rates where more sodium is transported over the cyclic scan (Fig. 3a).

Surprisingly, the Na/Na cell in which the sodium working electrode was saturated with excess Na_2O, did not show any evidence of asymmetric polarization at 350°C (however, this cell exhibited considerable polarization at lower temperatures).

Low Temperature (160 to 240°C): - The current-potential curves appeared to be extremely sensitive to the presence of oxygen or water at these temperatures. Asymmetric polarization was generally observed in this temperature range, and only under certain conditions could it be eliminated.

Filtered Sodium: - With filtered sodium used as a working electrode, the asymmetric polarization at 200°C was considerable. As Fig. 4, the resistance, R_i, is constant form + 100 to + 300 mV on the reverse scan, and increases in the region + 300 to 0

mV on the forward scan. R_i decreases rapidly as the potential moves into the negative region 0 to -300mV on the forward scan, slowly increases in the range - 300 to -50 mV on the reverse scan, and rapidly increases as the potential goes through 0 mV on the reverse scan. The maximum change in the resistance over the cyclic scan is 430 milliohms.

Filtered sodium + Ti - When titanium sponge was added to the working electrode of the cell described above a marked difference in the electrochemical behavior was observed. The asymmetry observed at positive potentials in Fig. 4 was completely removed, so that an essentially flat ohmic response was observed from + 250 mV to well into the negative potential region of the forward scan, Fig. 5. The resistance dropped sharply at about -100 mV, then rose again after the scan direction was reversed and the potential became less negative. The striking feature of Fig. 5 is that the large change in resistance occurs in the negative potential region of the cyclic scan, i.e. sodium flowing into the electrolyte tube (impurity concentrations decreasing at the interface). Also of note is that upon addition of Ti to the working electrode the change in the resistance over the potential scan had been reduced from 430 to 340 milliohms.

Sodium saturated with Na_2O - The cyclic voltammagrams and resistance-potential curves for this cell appear to be more complex, Figs. 6,7; in both cases was the asymmetric polarization quite significant. At 240°C (fig. 6) the resistance was increasing dramatically over the entire positive potential region regardless of scan direction. When the forward scan passes

into negative potentials the resistance decreases at a rate about 3 times faster than it was increasing at positive potentials. An obvious effect of the excess oxide in this cell was the large change in resistance over the course of the cyclic scan, R_i = 463 milliohms, larger than that observed at almost 100°C lower temperature.

When the temperature of this cell was lowered to 160°C, the observed behavior became more complex (fig. 7). The interface resistance was continually increasing over the extent of the reverse scan, and decreasing over the forward scan. Some features of the resistance-potential curves are particularly noteworthy. On the forward scan in the positive potential region the resistance is decreasing while sodium is still being passed out of the tube (oxide concentration increasing at the interface), and the large changes in resistance occur as the potential inflects through zero volts. The magnitude of the resistance change over the cyclic scan is quite large, R_i = 3000 milliohms, much larger than was seen for any other cell in this study.

Electrolyte exposed to moisture, (electrolytic sodium) - For this cell the electrochemical behavior was fairly simple. The resistance was relatively constant in the positive potential region, showing no asymmetry. The asymmetric changes in resistance were essentially observed at negative potentials; the magnitude of change being relatively small, R_i = 20 milliohms. The shape of the resistance - potential curve was analogous to

Figure 5.

Electrolytic sodium, and sodium reacted with Ti - For these cells asymmetric polarization was entirely absent over the whole temperature range, regardless of the scan rate or potential range, Fig. 8. Figures 4, 5, and 8 show the progressive elimination of the asymmetric polarization as oxide is removed from the sodium electrode in the same cell. Also evident in Figure 8 is that the presence of Ti in the sodium working electrode served to lower further the observed resistance 12 hours later. While dismantling these cells it was also observed that the beta"-alumina tubes were extremely well wetted by the sodium. These experiments demonstrate that asymmetric polarization at the sodium/beta"-alumina interface can be eliminated by use of totally dry beta"-alumina electrolyte in combination with either an electrolytic or oxygen reduced sodium electrode.

DISCUSSION

From the results of the above experiments it is obvious that the presence of oxygen and/or water significantly modifies the electrochemistry of the sodium/beta"-alumina interface. This is particularly evident at lower temperatures. The resistance polarization observed in these experiments is most likely due to the formation of a film or adsorption layer which is resistive to the transfer of sodium ions. As we have no way of directly observing the electrode/electrolyte-interface during the course of these experiments we can only infer the nature of this resistive layer from its electrochemical behavior.

In all cases where asymmetric polarization was observed, was the resistance higher at positive potentials, sodium was exiting the tube and the concentration of impurites was increasing at the working electrode interface. The largest changes in resistance occured as the potential inflected through zero volts, or at negative potentials well beyond zero volts (Fig. 5). The simplest explanation would be that the growth of the resistive layer is directly linked to the changes in oxide concentration as sodium is electrolysed either in or out of the electrolyte tube.

Oxygen Depletion and Adsorption Model - The relative change in the concentration dissolved oxygen at the Na/beta"-alumina interface as a function of time and current density can be calculated using the model of De Jonghe and Hitchcock[14]. At negative potentials, pure, oxide-free sodium is formed at the working electrode/electrolyte interface. Conversely, at positive potentials pure sodium is removed from the interface, leaving impurities behind. As the oxide is swept either away from or toward the electrolyte surface a concentration gradient is established and diffusion of oxygen occurs in the opposite direction. The oxygen concentration follows the equation of convection and diffusion; which in one dimension is

$$dc/dt = D(d^2c/dx^2) - v(dc/dx) \qquad (1)$$

where D is the diffusion coefficient of oxygen in molten sodium, v is the sodium velocity, and x is the distance from the electrolyte surface. The problem has been solved by

Mason and Weaver[15], and the solution is:

$$C/C_0 = \frac{-v\sqrt{t}}{\sqrt{D\pi}} \exp - [(vt - x)^2/4Dt] + \tfrac{1}{2}[1 - \mathrm{erf}(\frac{vt - x}{\sqrt{4Dt}} + \tfrac{1}{2}\exp(\frac{vx}{D})[1 + \frac{v}{D}(vt + x0][1 - \mathrm{erf}(\frac{vt + x}{\sqrt{4Dt}})] \quad (2)$$

where C_0 is the initial concentration for all x.

The diffusion coefficients for oxygen in molten sodium are not reported in the literature. If the significant asymmetric polarization observed at lower temperatures (160-200°C) is in fact due to changes in the oxide concentration at the electrode/electrolyte interface, then the diffusion of oxygen in molten sodium must be quite slow. The diffusion of oxygen in liquid indium has been measured. Since the self-diffusion rates and heats of formation of the oxides of both sodium and indium are nearly the same, the equation of Klindinst and Stevenson[16] for the diffusion of oxygen in molten indium is used to estimate a value of D at the low temperature extreme. One calculates a value of D equal to 1×10^{-14} m^2/s at 160°C. The model of De Jonghe and Hitchcock[14] for the mechanism of slow crack growth in "-alumina is consistent with an oxygen diffusion coefficient in molten sodium of 5×10^{-9} m^2/s at 300°C. For the purpose of making rough calculations, the above values of D at 160 and 300°C can be used to construct a table of estimated diffusion coefficients, as shown in Table 2. By inspection one can see that due to the temperature dependance of the diffusion coefficient, the values of C/C_0 calculated from Eqn. 2 will be very sensitive to temperature; C/C_0 will change much more rapidly(under conditions of equal t and v) at the electrode/electrolyte

interface at 160°C than at 300°C. This may explain why such large asymmetry is observed at low temperatures and not at high temperatures.

Approximate calculations of C/C_0 can be made for the changes in oxide concentration at the Na/beta"-alumina interface for the cyclic voltammograms in this study. Since the current density is not constant but rather a function of the potential and resistance, C/C_0 at the interface (x=0) can be calculated over small time intervals assuming constant current over that interval. In most cases the decrease in C/C_0 was calculated for the forward cathodic current scan, but the increase in C/C_0 on the anodic scan is just as easily calculated. Since C/C_0 is dependant on both v and t, there should be a strong dependance on scan rate. Qualitatively, this is always observed; the asymmetry is most severe at low scan rates (for the same potential region) where more current is passed.

The change in C/C_0 is shown in Figure 9 for a constant cathodic current density of 30 mA/cm2 at the two temperatures of 160°C and 300°C. As one can clearly see, the drop in solute concentration at the electrode/electrolyte interface is far more rapid at 160°C. As discussed previously in the results section, asymmetric polarization is seldom observed at high temperatures. The lack of significant change in C/C_0 at 300°C Fig. 9 may provide an explanation for this effect.

The effect of scan rate at low temperatures on the resistance-potential evolution and on the change in C/C_0 is shown

in Figures 10 and 11, respectively. One can easily see that the magnitudes of both the asymmetric polarization and the change in C/C_0 are much larger at the slower scan rate. At the end of the cathodic scan(0 to -250 mV) in Figure 10a, the oxide concentration is calculated to be 0.08 of the initial concentration. The equivalent depletion of oxide occurs for the slow scan at about -100 mV. In the first case the interface resistance has decreased by about 45 mohms, and in the latter case by 100 mohms.

The difference between these two cases is the time lapsed to achieve the value of C/C_0 = .08, five seconds in the rapid scan case, while about 50 seconds in the slow scan case. This implies that there is an additional kinetic step in the removal of the resistance at the electrode/electrolyte interface. This may be due to the desorption of an adsorbed oxide layer; the coverage of the surface being affected both by the oxide concentration at the surface and the rate constant for desorption.

One plausible explanation for the electrochemical observations in this study is therefore a chemical adsorption of oxide or hydroxide on the beta"-alumina surface, possibly followed by growth of an oxide or hydroxide layer at higher solute concentrations. Using Kroger-Vink notation:

1. $OH^- + Na_{Na}{}^x \longrightarrow NaOH_i\ (ads)^x + V_{Na}$

2a. $O^{2-} + Na_{Na}{}^x \longrightarrow NaO_i(ads) + V_{Na}$

2b. $NaO_i(ads) + Na_{Na}{}^x \longrightarrow Na_2O_i(ads)^x + V_{Na}$

3. NaOH or Na_2O film growth

where V =vacancy, $_{Na}$ =sodium site, $_i$ =interstitial, ^{x} =neutral,

and =negative charge.

In the presence of dissolved oxide or hydroxide in the molten sodium electrode, the beta"-alumina electrolyte could chemadsorb those species at the conduction planes by removing a sodium ion from a sodium ion site, yielding an adsorbed NaO^- or NaOH and a sodium ion vacancy in the beta"-alumina. One would expect this adsorption to increase the resistivity of the electrolyte both by trapping conduction ions and by blocking the flow of ions into and out of the electrolyte surface.

In the simple case of a Langmuir adsorption the degree of surface coverage will determined by the equilibrium constant for adsorption which is a function of the concentration of oxide at the interface (17)

$$\theta/1-\theta = (k_1/k_{-1})c = K_c \qquad \theta = K_c/(1+K_c)$$

where θ is the fraction of surface sites occupied, and K is the equilibrium constant or adsorption coefficient. As the value of K becomes very large (strong adsorption), the isotherm approaches the form of the unit step function, in other words, there is little dependance of θ on concentration. On the other hand, if K is small, θ is strongly dependant on adsorbate concentration.

As was discussed in the Results section, little if any asymmetry was observed at high temperatures. The heat of adsorption for chemisorption is typically in the range of 10 - 100 kcal/mole. For the Langmuir adsorption isotherm, the temperature variation of the equilibrium constant follows the van't Hoff relationship:

$$d\ln K/dT = -\lambda/RT^2$$

where λ is the heat evolved per mole of reactant in the adsorption process. If one uses a relatively small value for the heat of adsorption, say -20 kcal/mole, the ratio of the equilibrium constant K at 300°C, to K at 160°C is 0.0034. As one would expect, the adsorption is much less favored at high temperatures. Similarly, since the entropy change for adsorption is negative, the free energy change for the adsorption reaction is less favorable at high temperatures.

Therefore, there are two factors in this model that predict the absence of asymmetric polarization at high temperature: the change in solute concentration at the electrode/electrolyte is much less pronounced at high temperatures, and the equilibrium constant for adsorption should be much smaller at high temperatures.

A simple example of the asymmetric polarization observed at low temperatures is seen in Figure 5. The change in C/C_0 was calculated for the cathodic and anodic current ranges of this resistance-potential curve. The calculations were done assuming C/C_0 =1 at zero potential, and then over the range of zero volts to the positive or negative limit of the potential window(the reverse scans were not calculated).

The shape of the resistance-potential curve in Figure 5 is explained as follows. As the potential is scanned in the negative direction, the cathodic current increases in proportion to a constant resistance up to about -75 mV. At this point C/Co

has dropped to about 0.84, the oxide begins to desorb and the interfacial resistance begins to drop. As the potential scan is continued, the current density increases at a more rapid rate due to the falling resistance. The increasing current density causes C/C_0 to fall off more rapidly, causing the oxide film to further desorb. This synergistic effect would lead to the steep slope observed after the onset of the resistance drop. The resistance decrease appears to slow down near the limit of the potential scan implying that most of the film is desorbed. After the scan is reversed, the oxygen begins to diffuse back to the electrolyte surface due to the decreasing current density and the large concentration gradient established at the end of the forward scan. Between -300 mV and -150 mV there is little change in the resistance since the dissolved oxygen is still diffusing against significant convection. Readsorbtion becomes noticeable at potentials positive of -150 mV; the resistance starts to increase appreciably, decreasing the current density more rapidly, allowing enhanced back-diffusion of oxide to the electrolyte surface and formation of the oxide film. The film is essentially re-established at zero volts, and the resistance does not increase as the potential is scanned into the positive region even though C/C_0 increases to 2.4 by the end of the forward positive scan, indicative of maximum coverage).

If Figures 4 and 5 are superimposed, one can see an additional feature in Figure 4: an increasing resistance which initiates at the point at which the direction of the triangular potential scan is reversed. If this additional resistance is due

to a second chemical adsorption step, it's odd that it doesn't appear when the anodic scan passes into the positive potential region, but rather intiates where the scan direction is reversed (C/C_0 is maximum here) at the positive potential limit. Possibly the second chemical adsorption is nucleated by the scan direction reversal, due to the capacitive effect of a rapid reversal of current flow through the double layer as dV/dt changes sign. This feature would not show up in Figure 4, since the sodium in this case was treated with Ti, removing the species(possibly hydroxide) responsible for this observation.

The extreme case of oxide contamination is that of electrolytic sodium saturated with Na_2O. Since the oxide concentration is at the solubility limit,during anodic current flow C/C_0 should remain unity while sodium flows into the electrolyte, leaving oxide behind to either adsorb on the electrolyte surface (possibly followed by a growing sodium oxide layer), or precipitating out of the molten sodium. In figure 6 the resistance at the interface is observed to increase over the entire positive potential region. Since the oxide concentration is at the solubility limit, and therefore adsorption coverage is probably already maximum, the increase in resistance could be due to the buildup of a Na_2O film as excess oxide is deposited at the interface during anodic current flow. This hypothesis is supported by the results seen in Figure 7. There is an enormous increase in the interface resistance with anodic current flow, 3 ohms, which is 2 orders of magnitude larger than for unsaturatred sodium at 160°C.

This indicates that there might be two mechanisms for resistance rise at the electrode/electrolyte interface: adsorption of oxide or hydroxide at the interface, and buildup of an oxide film at saturation concentrations (Fig. 12).

At the lower concentration extreme, electrolytic sodium or sodium treated with Ti and filtered there is little, if any, evidence of asymmetric polarization over the entire temperature range, Fig. 8. There are no indications of adsorption in these cases even at 160°C where there are large changes in C/C_0 over the course of the cyclic voltammograms.

CONCLUSIONS

The introduction of oxygen in the form of either dissolved O_2 or H_2O into the sodium electrode of a Na/Na cell leads to asymmetric polarization. The observed polarization is most severe below 300°C, and is quite large in the range of 150-200°C. The increased interfacial resistance is attributed to the chemisorption of an oxide or hydroxide layer at the conduction planes of the beta"-alumina electrolyte. This may be followed by the growth of an Na_2O or NaOH film (evidenced by a very large asymmetry) at impurity concentrations exceeding the solubility limit in molten sodium. The adsorption mechanism can be approximately described by a simple Langmuir adsorption model. The asymmetric polarization is then visualized as an adsorption/desorption governed by changes in the concentration of dissolved oxygen, at the electrolyte surface, as described by the

equation of diffusion and convection.

The asymmetric polarization can be effectively eliminated by the use of carefully dried electrolyte tubes in combination with either electrolytic sodium or sodium from which the oxygen has been scavenged with titanium sponge and filtered.

ACKNOWLEDGEMENTS

This work was supported by the Assistant Secretary for Conservation and Renewables, Office of Advanced Conservation Technology, Electrochemical Systems Research Division of the U. S. Department of Energy under Contract No. DE-AC03-76SF000098.

REFERENCES

1. M. W. Breiter, B. Dunn and R. W. Powers, Electrochem. Acta, 25, 613 (1980).

2. M. W. Breiter and B. Dunn, ibid., 26, 1247 (1981).

3. D. S. Demott, J. Electrochem. Soc., 127, 2312 (1980).

4. W. Jukubowski and D. H. Whitmore, J. Amer. Cer. Soc., 62, 381, (1979).

5. R. J. Bones and T. L. Markin, J. Electrochem. Soc., 125, 1587 (1978).

6. J. L. Sudworth, A. R. Tilley, and K. D. South, Fast Ion conduction, Van Gool (1972).

7. H. U. Borgstedt, "liquid Metal Systems", Plenum Press, NY (1973).

9. C. Jackson, "Liquid Metals Handbook, Sodium (NaK) Supplement", U. S. Government Printing Office, D. c. (1950).

10. H. Ullman, "Liquid Metals Systems", pg. 375, Plenum Press, NY (1982).

11. C. A. Smith and A. C. Whittingham, ibid., pg. 365.

12. M. Sittig, "Sodium, it Manufacture, Properties and Uses", pg. 374, Reinhold Pub. Corp. (1956).

13. Barak, "Electrochemical Power Sources", pg. 443., Inst. Elec, Eng. (1980).

14. L. C. De Jonghe and D. Hitchcock, J. Electrochem. Soc., 133, 6(1986).

15. M. Mason and W. Weaver, Phys. Rev., 23, 412(1924).

16 K. A. Klinedinst and D. A. Stevenson, J. Electrochem. Soc., 120, 304 (1973).

17 W. J. Moore, "Physical Chemistry", Fourth Edition, Prentice Hall (1972).

FIGURES

Figure 1. Sodium/sodium cell used in cyclic voltammetry studies.

Figure 2. Simplified equivalent circuit for the Na/Na cell.

Figure 3a. Cyclic voltammogram of Na/Na cell at 350 C showing slight asymmetric polarization; 1 mV/sec; - - - 20 mV/sec. Note deviation from ohmic behavior is larger at slower scan rates 3b. Corresponding resistance-potential curve for 1mV/sec scan rate showing calculated points and least squares lines; - - - forward scaan; - - - reverse scan. Note decreasing resistance as forward scan 0 millivolts.

Figure 4. Resistance-potential curve; 200 C; filtered sodium; scan rate = 20 mV/sec; forward scan; - - - reverse scan.

Figure 5. Resistance-potential curve; 200 C; filtered sodium plus titanium sponge; scan rate = 20 mV/sec; forward scan; - - - reverse scan.

Figure 6. Resistance-potential curve; 240 C; sodium electrodes saturated with Na_2O; scan rate = 20mV/sec; forward scan; - - - reverse scan.

Figure 7. Resistance-potential curve; 160 C; sodium electrodes saturated with Na_2O; scan rate = 20 mV/sec; forward scan; - - - reverse scan.

Figure 8. Resistance-potential curve; 200 C; filtered sodium reacted with titanium sponge at 350 C overnight; scan rate = 1 mV/sec; initial cyclic scan; - - - cyclic scan 24 hours later. Note complete absence of any asymmetrik polarization.

Figure 9. Oxygen depletion model. Ratio, C/C_0, of dissolved oxygen at the electrolyte surface to the bulk concentration as a function of time and temperature.

Figure 10. Resistance potential curves; 160 C; electrolytic sodium wtih slight oxygen contamination; scan rate = 50 mV/sec 2mV/sec; forward scans; - - - reverse scans.

Figure 11. Oxygen depletion at electrolyte surface calculated for the cell depicted in Figure 10 over the potential interval of 0 to -250 millivolts for the forward scan; the time interval is determined by scan rate; 50 mV/sec; - - - 2 mV/sec. At the end of the potential interval (0 to -250 mV) C/C_0 has dropped to 0.08 for the fast scan case and 5×10^{-8} for the slow scan case.

Figure 12. Oxygen contamination levels of the sodium electrode and associated phenomena.

TABLE 1

Temperature (°C)	Solubility of Oxide from Na_2O (ppmO)	from H_2O (ppmO)	from NaOH (ppmOH)
350	215	557	6084
300	97.6	212	2312
200	12.2	16.6	124
160	4.1	4.3	46.9
100	0.50	0.33	26.3

XBL 862-690

TABLE 2

Temperature (°C)	Diffusion Coefficient (m^2/sec)
300	5×10^{-9}
200	1×10^{-12}
160	1×10^{-14}

XBL 862-689

Figure 1

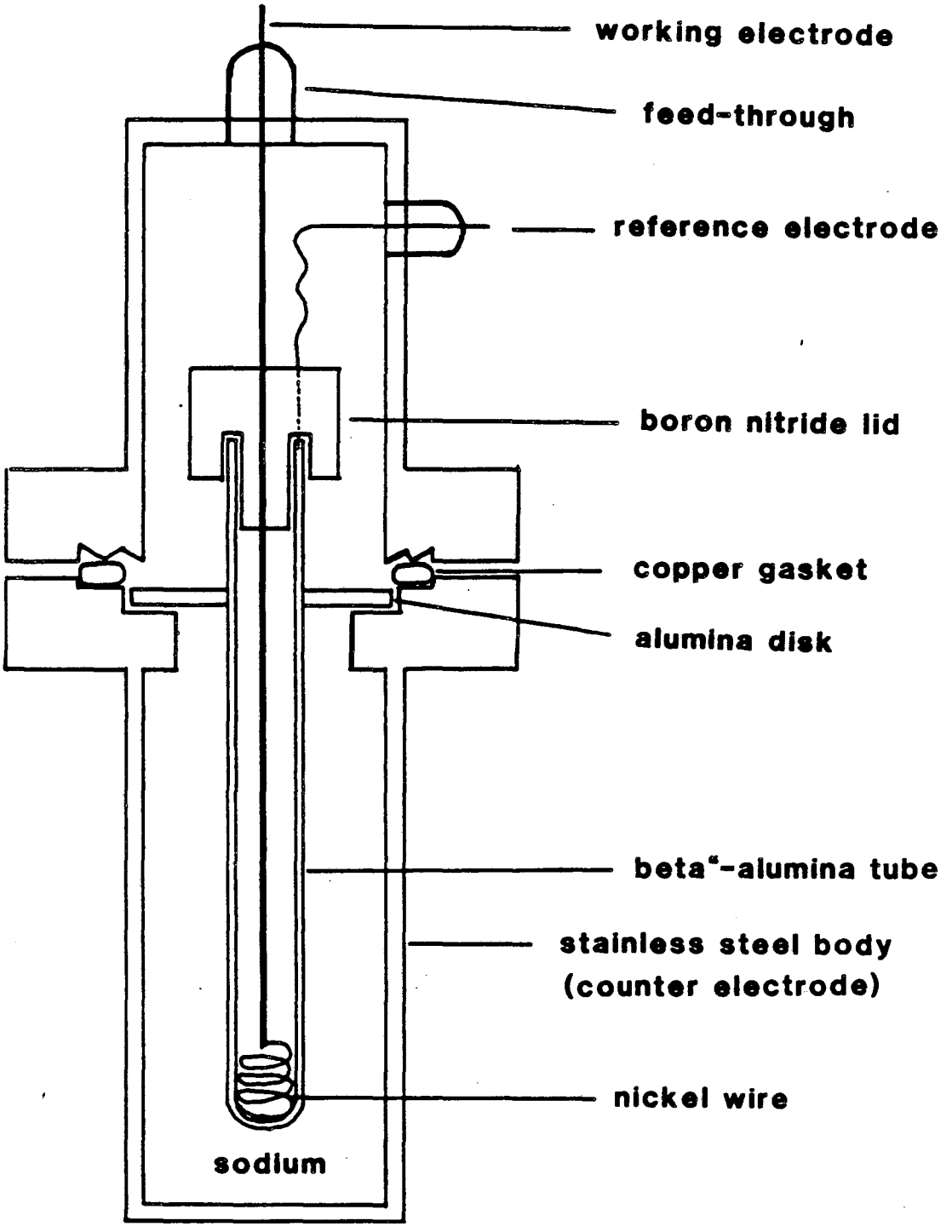

XBL 862-687

Figure 2

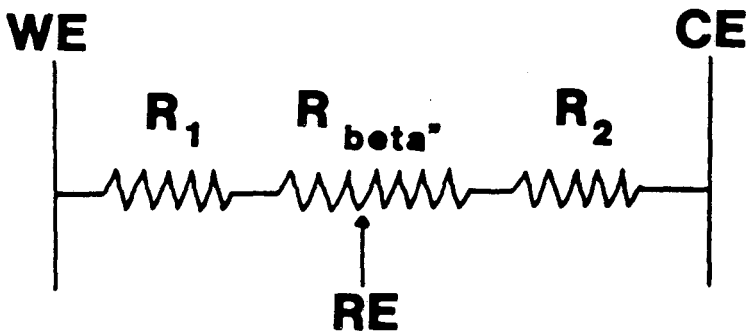

XBL 862-691

Figure 3a

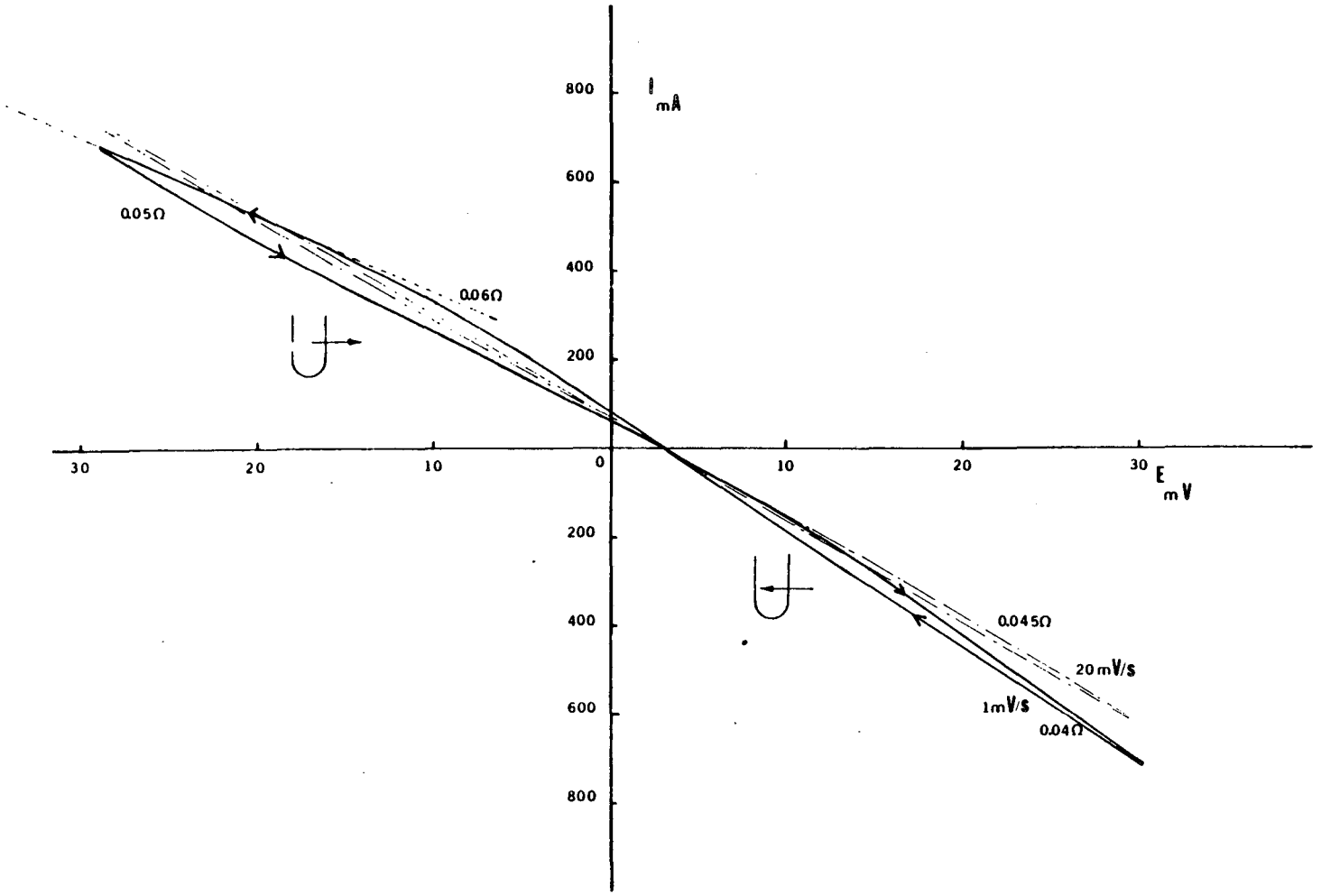

XBL 862-686

Figure 3b

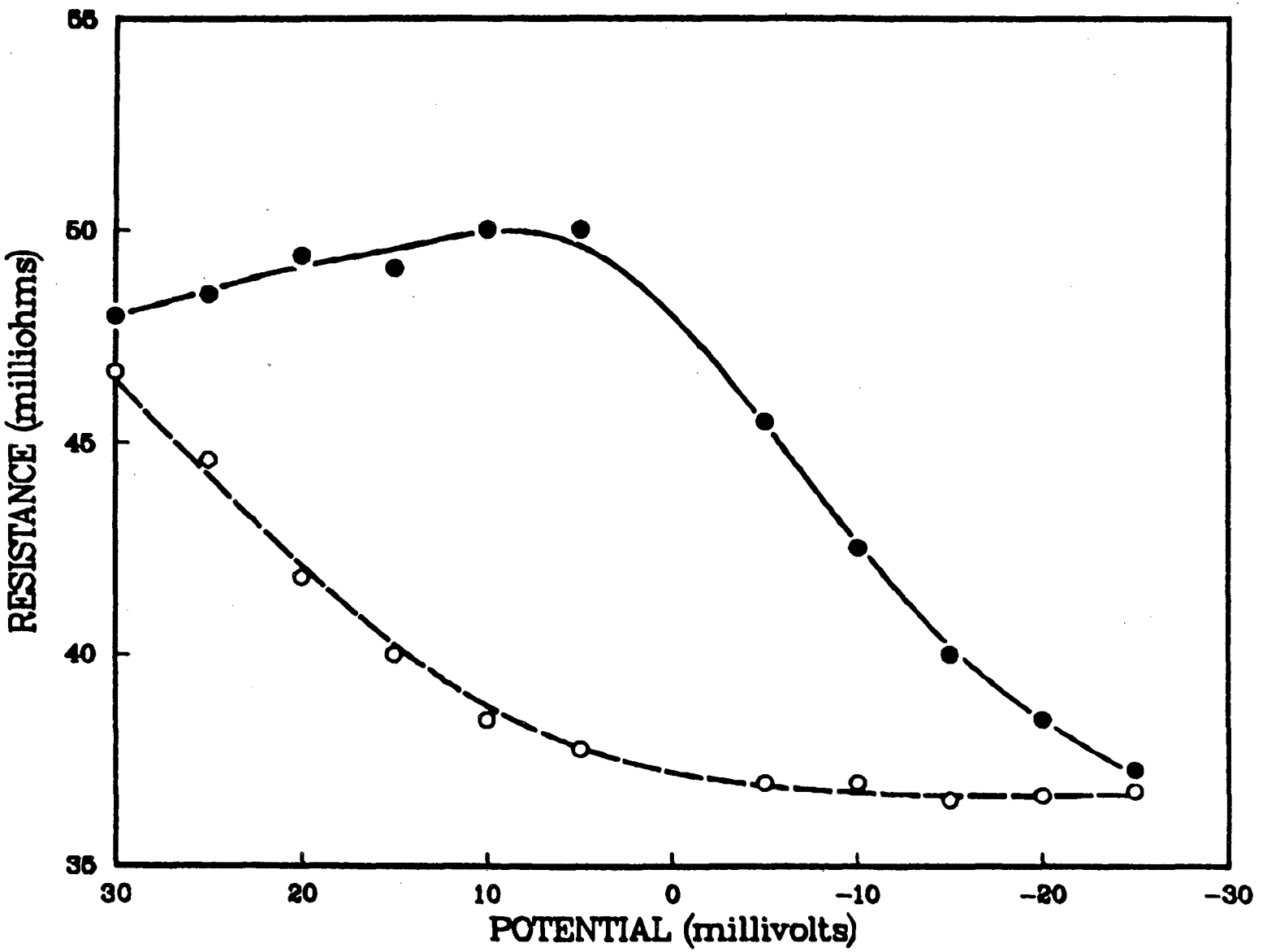

XBL 862-677

Figure 4

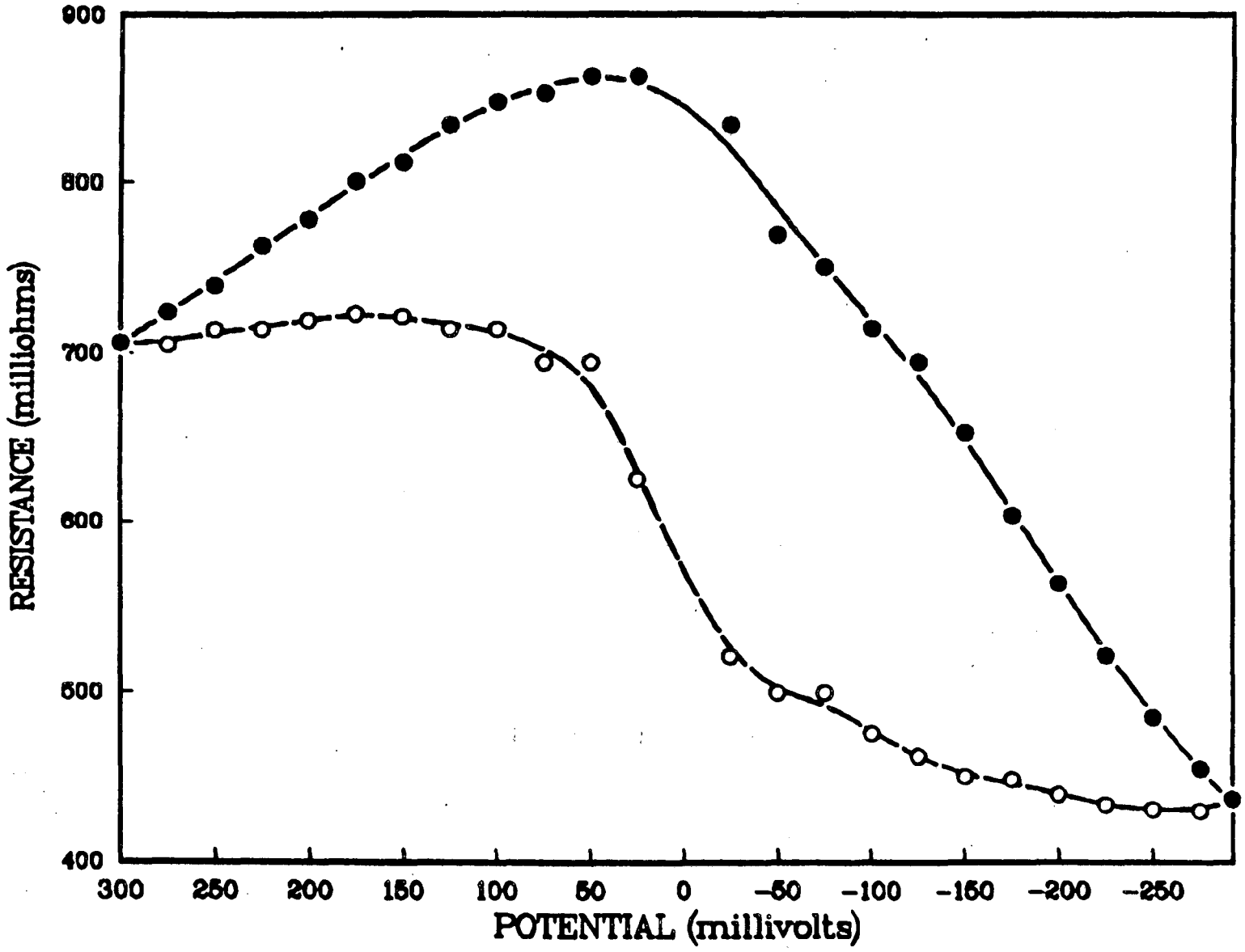

XBL 862-678

Figure 5

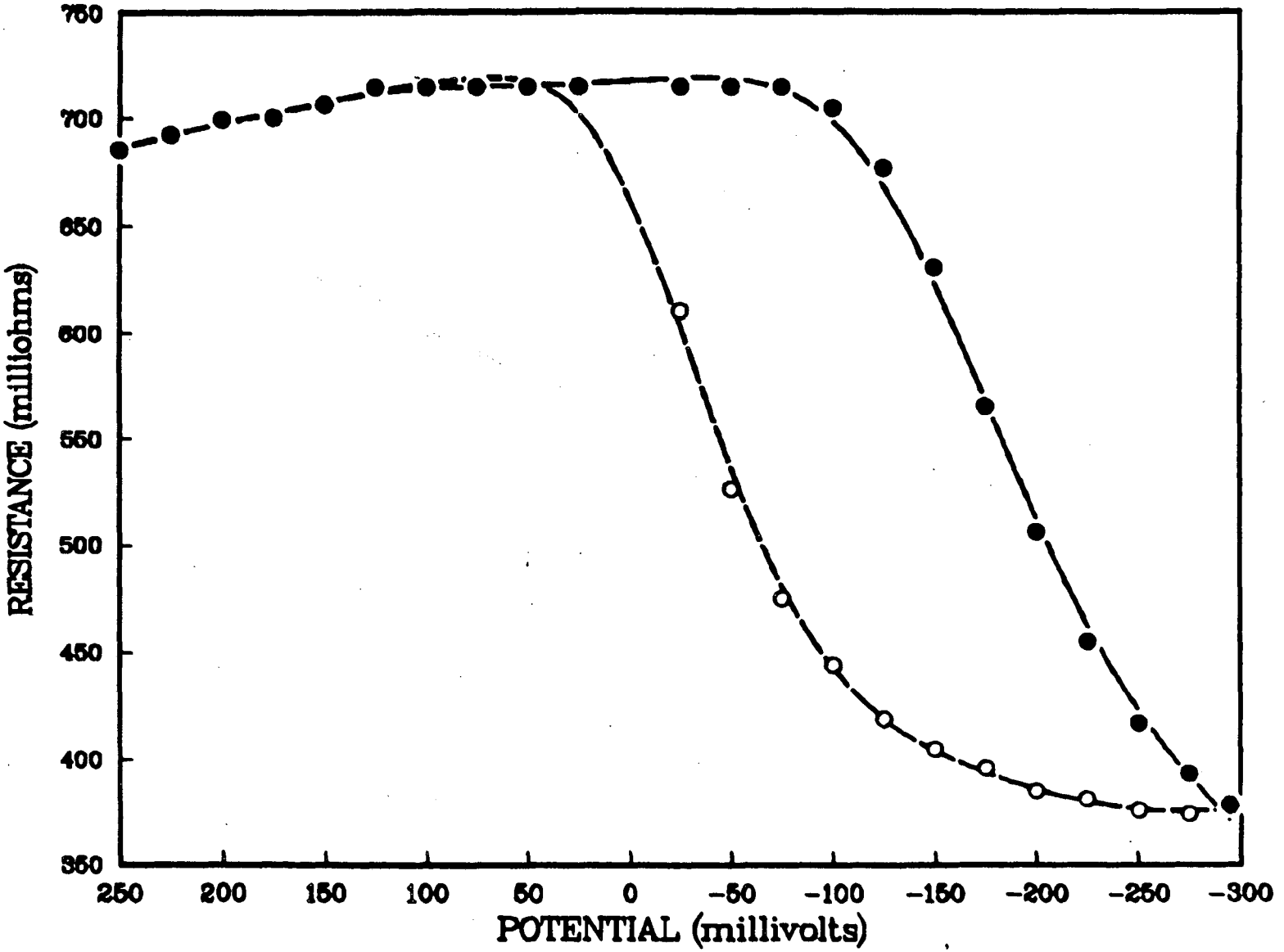

XBL 862-679

Figure 6

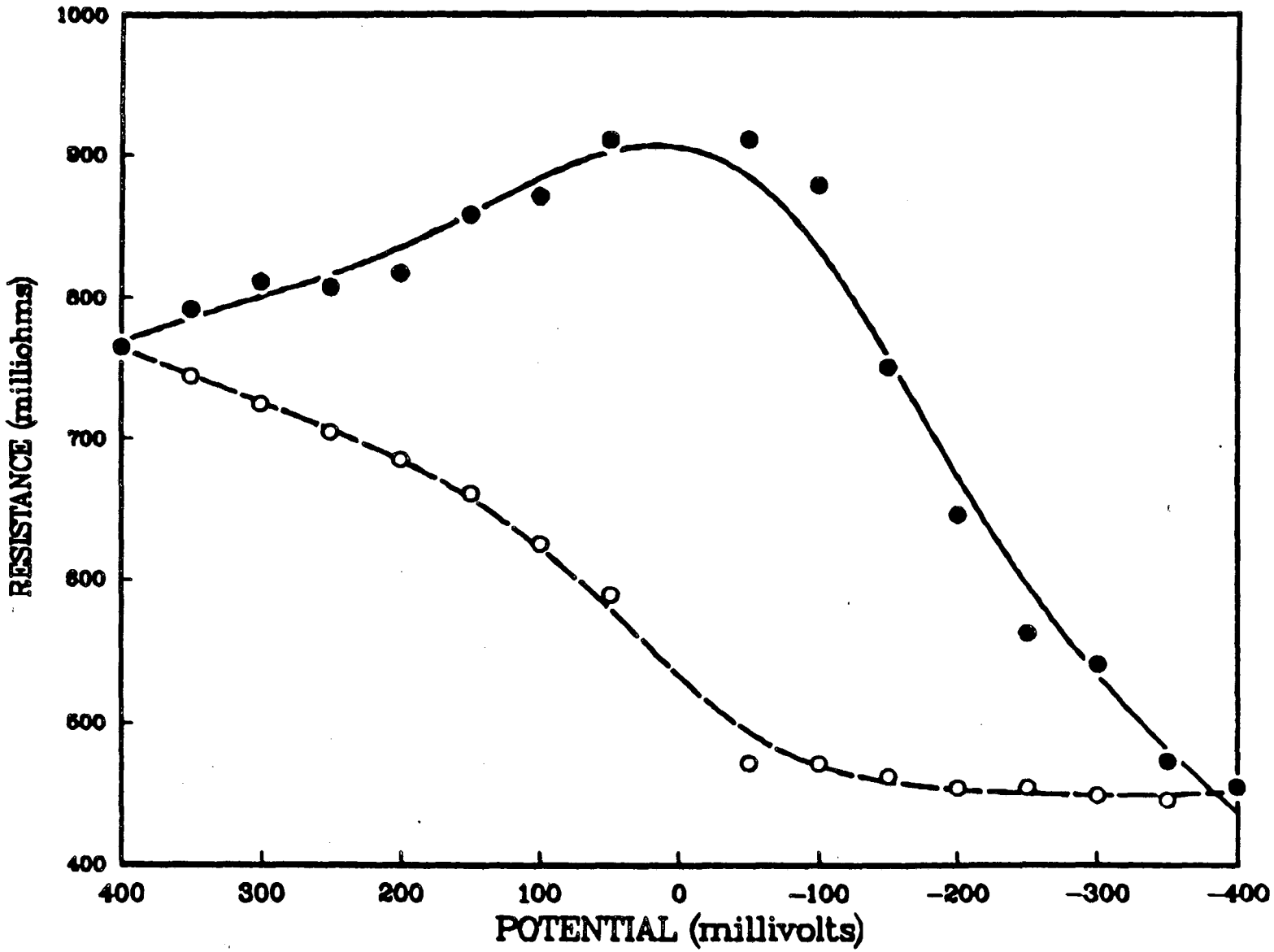

XBL 862-680

Figure 7

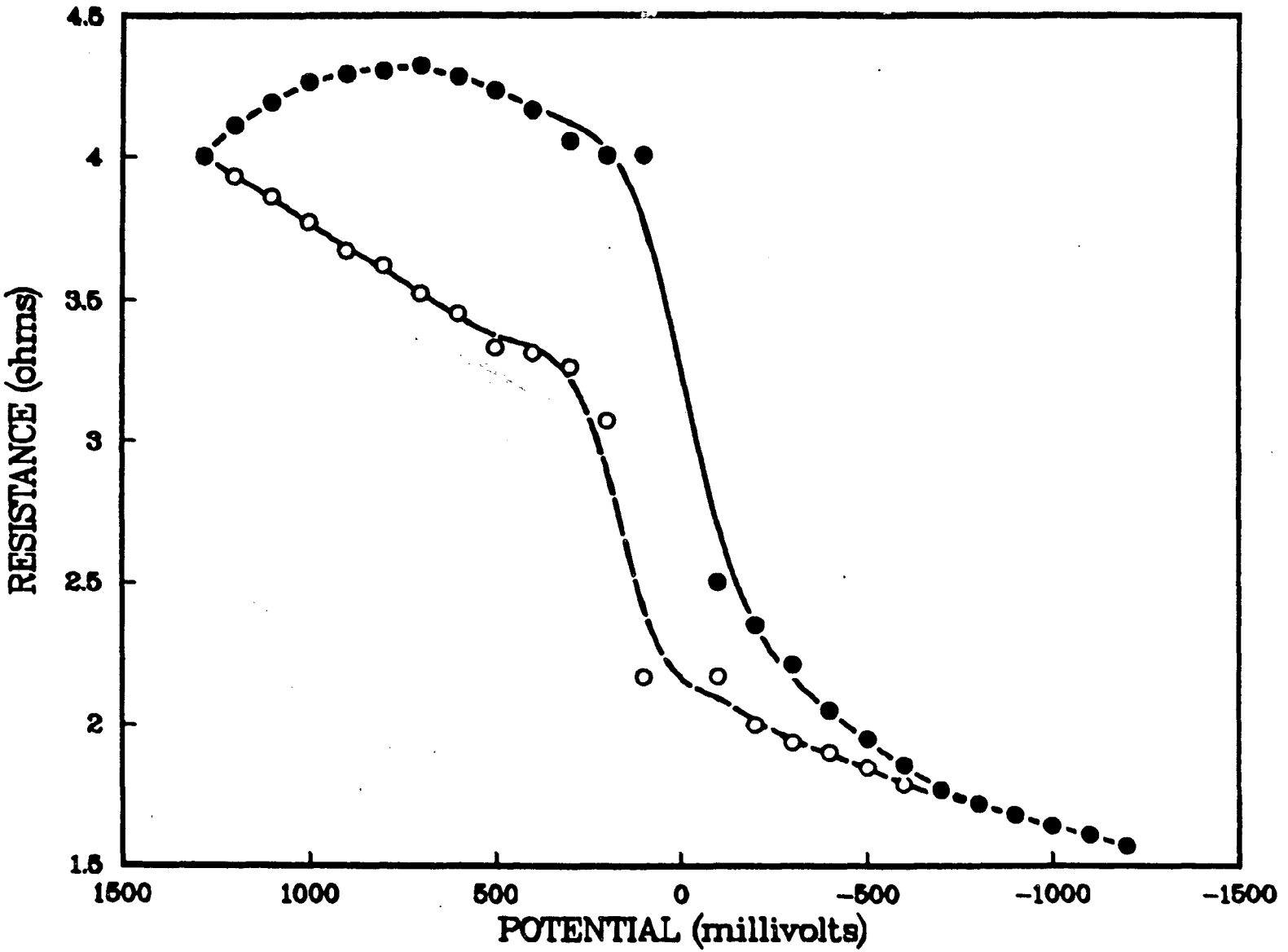

XBL 862-681

Figure 8

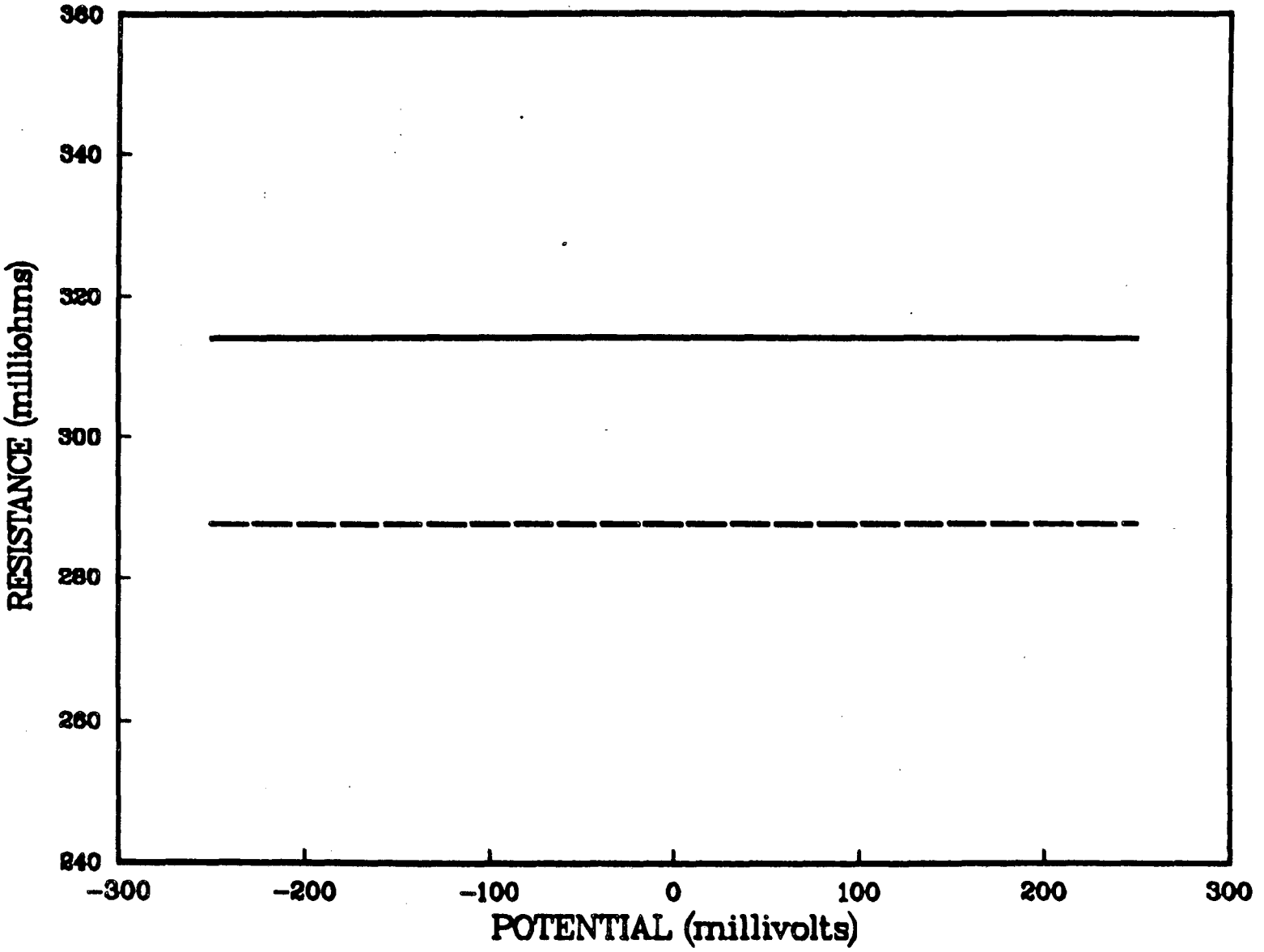

XBL 862-682

Figure 9

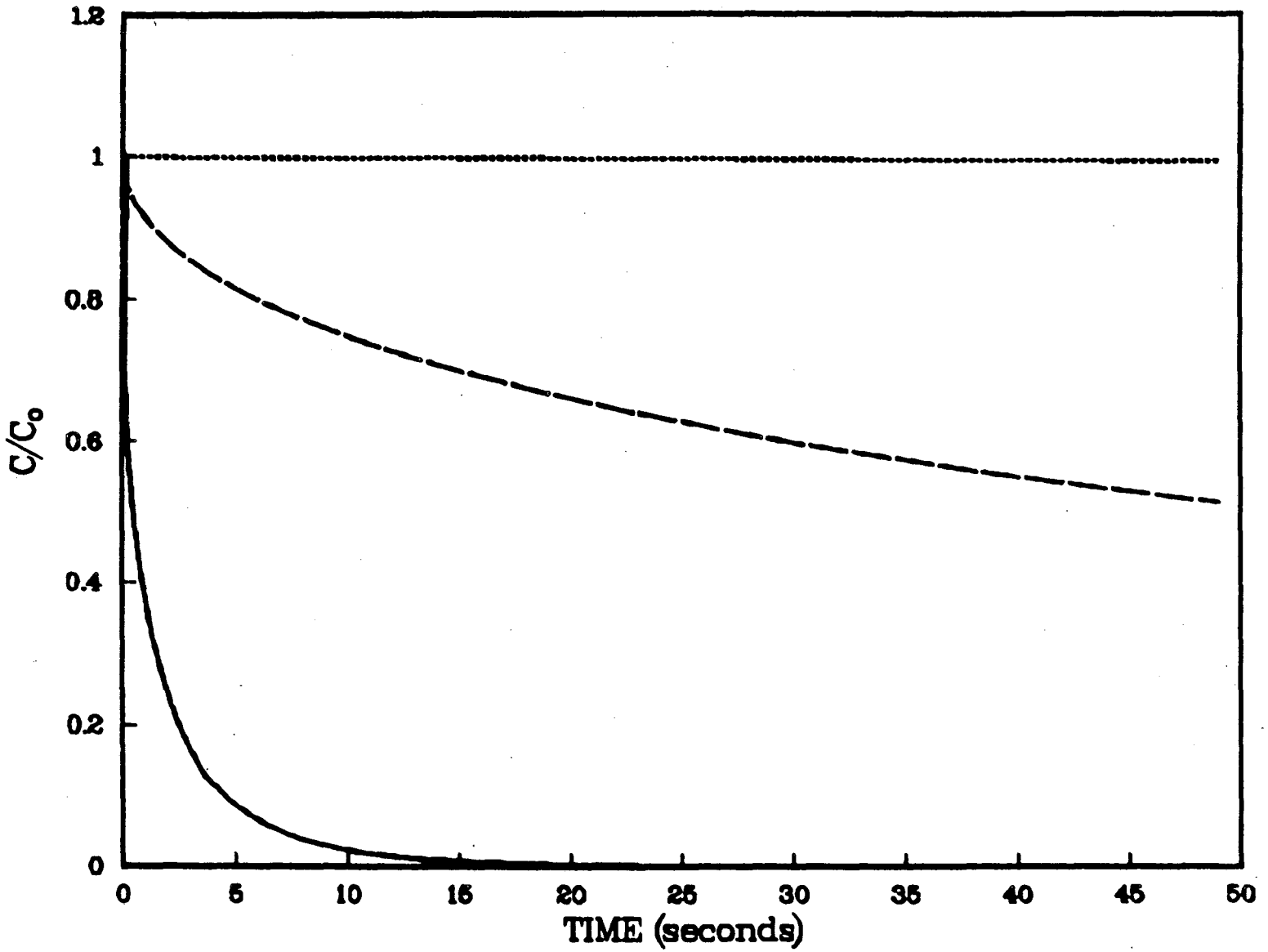

XBL 862-683

Figure 10

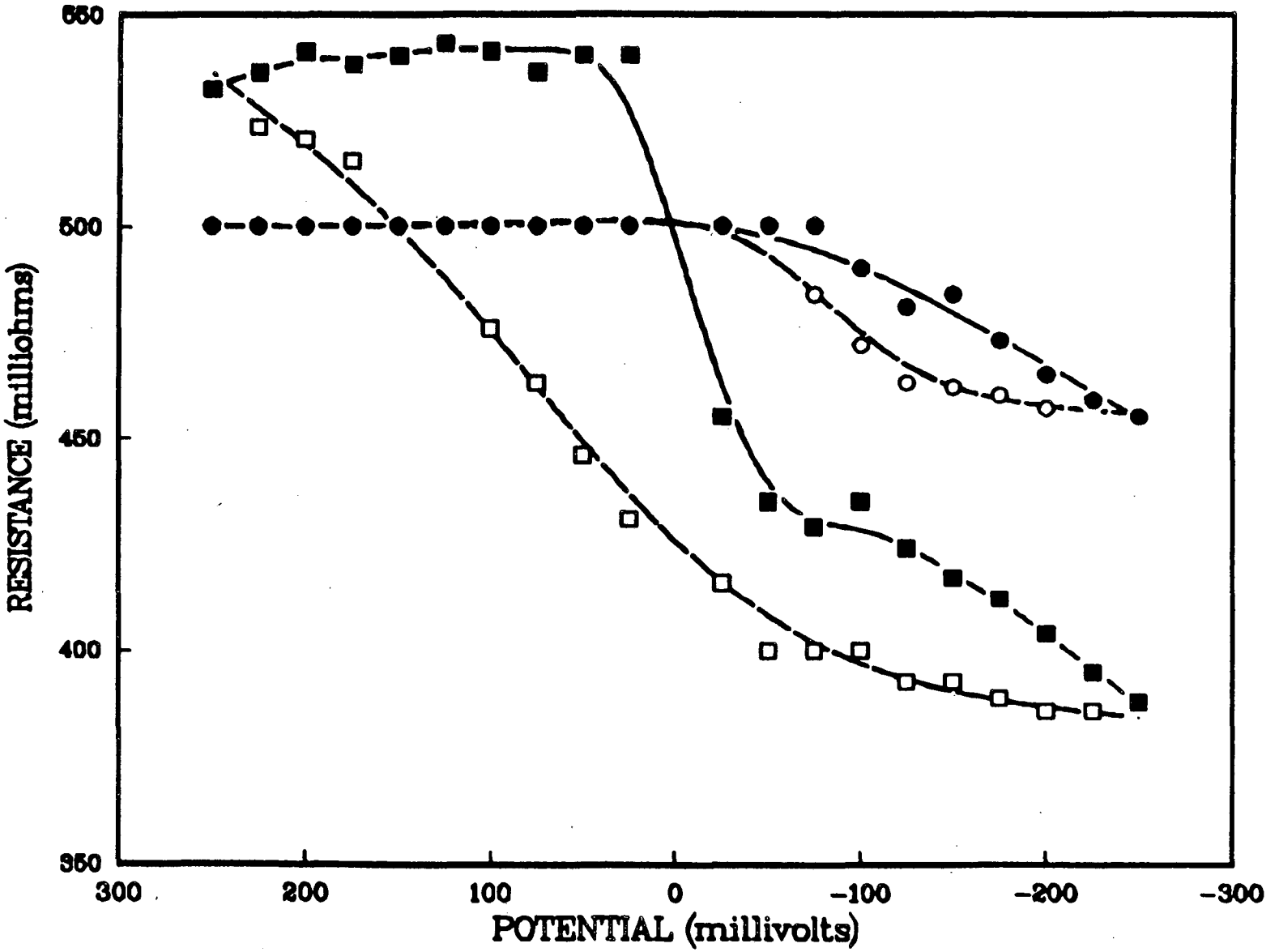

XBL 862-684

Figure 11

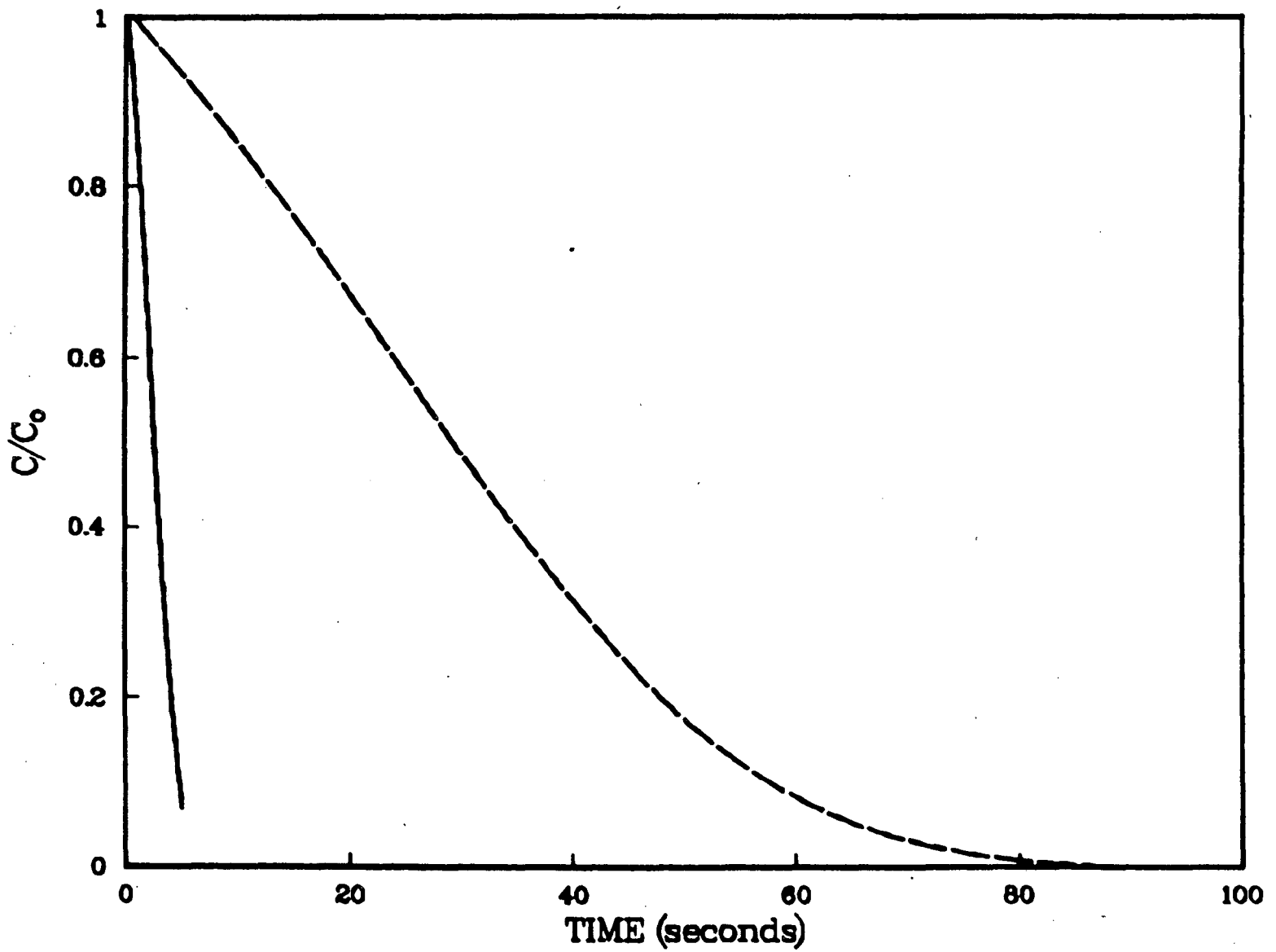

XBL 862-685

Figure 12

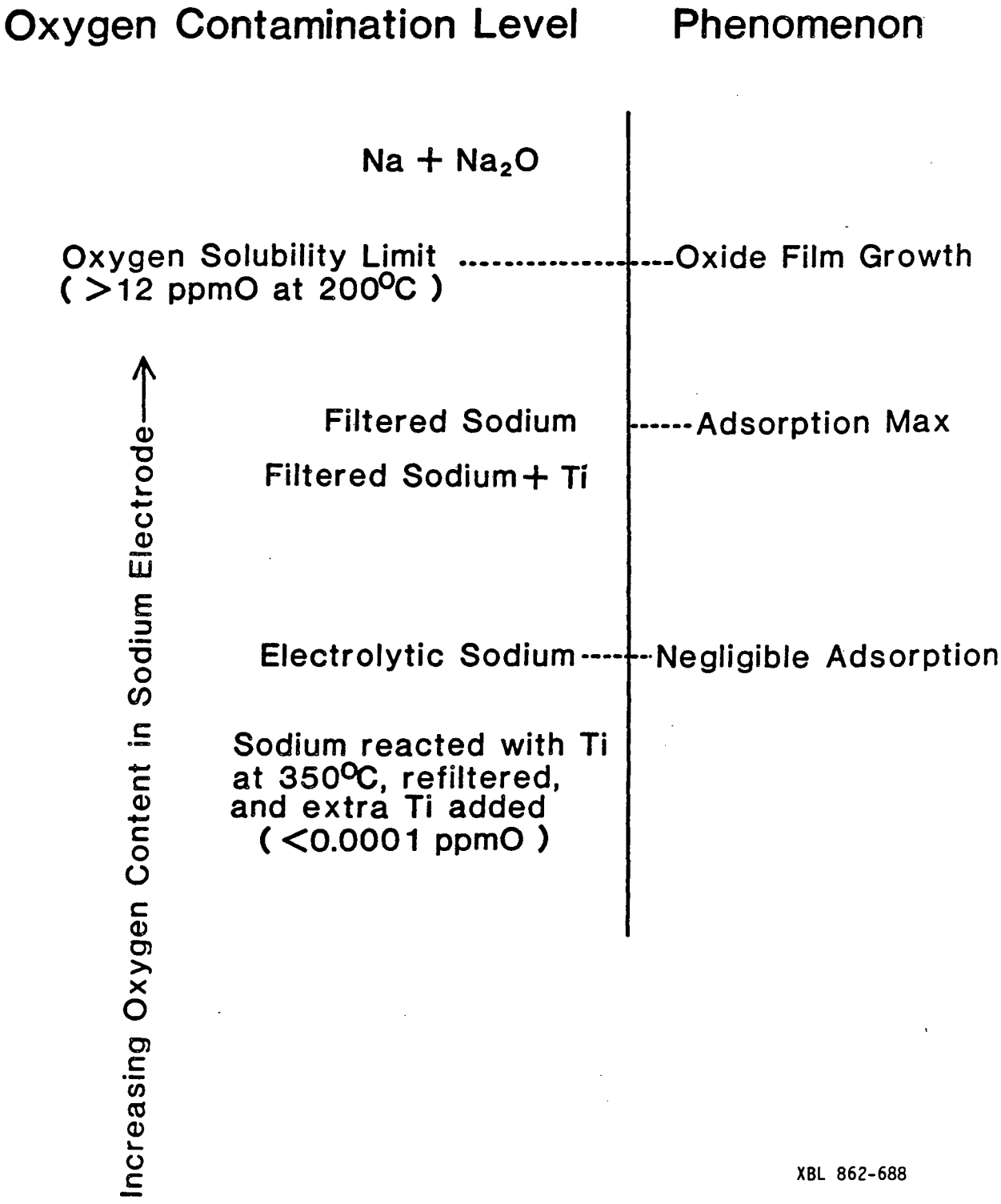
Oxygen Contamination Level
Phenomenon
Na + Na2O
Oxygen Solubility Limit
(>12 ppmO at 200°C)
Oxide Film Growth
Filtered Sodium
Filtered Sodium + Ti
Adsorption Max
Electrolytic Sodium
Negligible Adsorption
Sodium reacted with Ti
at 350°C, refiltered,
and extra Ti added
(<0.0001 ppmO)
Increasing Oxygen Content in Sodium Electrode
XBL 862-688

This report was done with support from the Department of Energy. Any conclusions or opinions expressed in this report represent solely those of the author(s) and not necessarily those of The Regents of the University of California, the Lawrence Berkeley Laboratory or the Department of Energy.

Reference to a company or product name does not imply approval or recommendation of the product by the University of California or the U.S. Department of Energy to the exclusion of others that may be suitable.

LAWRENCE BERKELEY LABORATORY
TECHNICAL INFORMATION DEPARTMENT
UNIVERSITY OF CALIFORNIA
BERKELEY, CALIFORNIA 94720